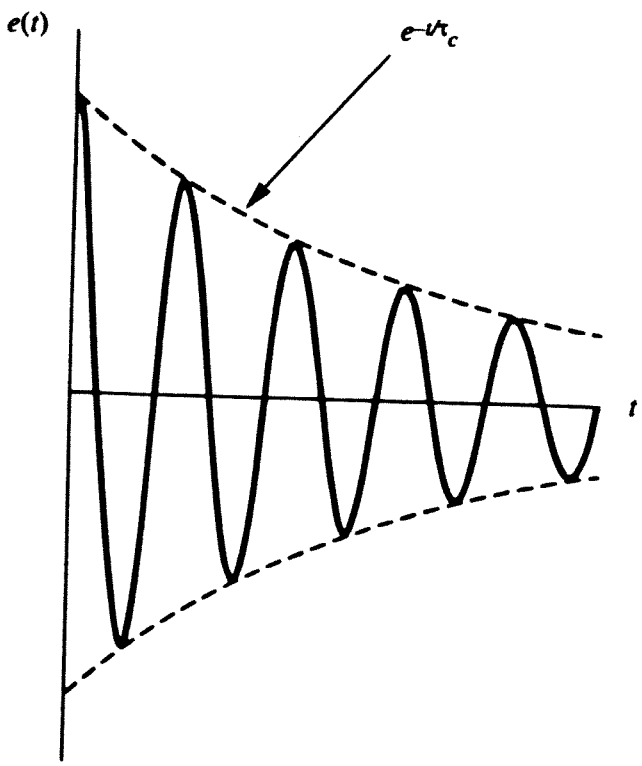

Fig. 2.1. The damped oscillation of the electric field produced by an excited particle as it decays.

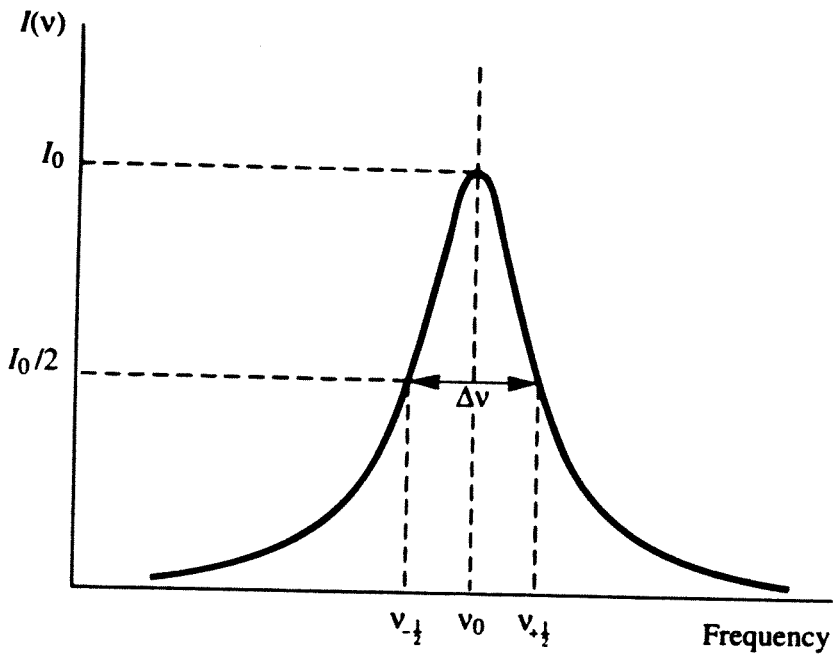

Fig. 2.2. Lorentzian lineshape function for natural broadening.

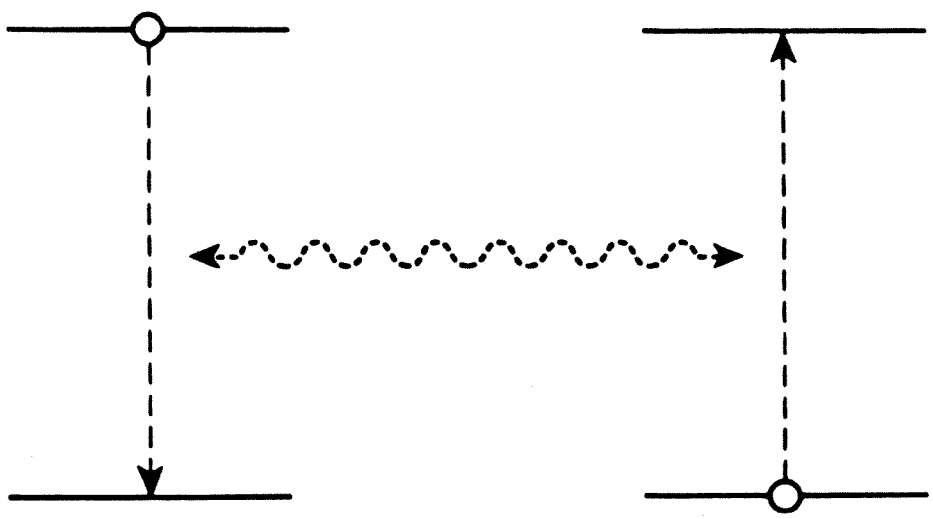

Fig. 2.3. Schematic illustration of how resonance and Van der Waals broadening arise.

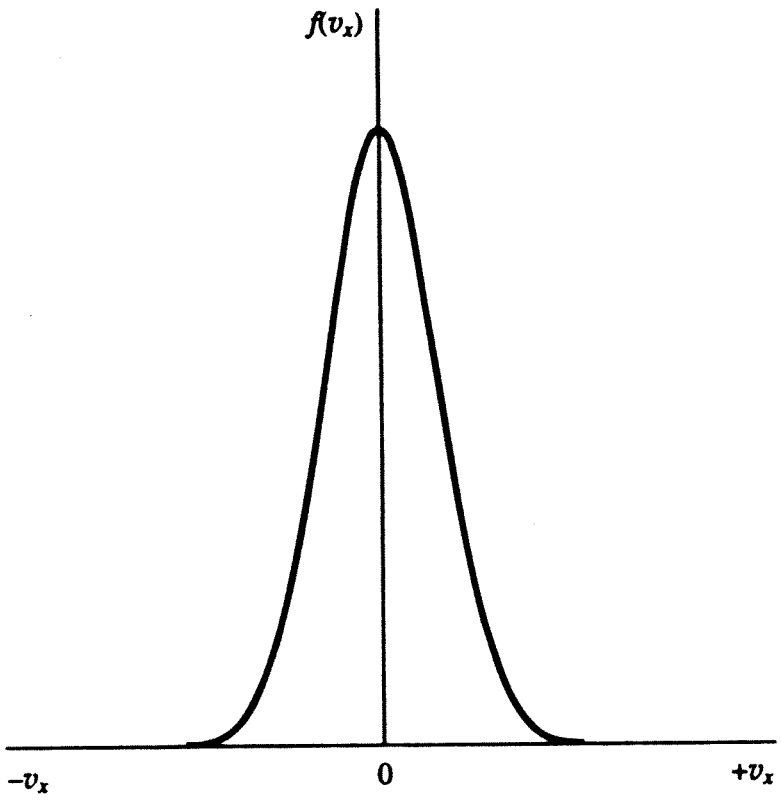

Fig. 2.4.
The one-dimensional Gaussian distribution of velocities for the particles in a gas.

Fig. 2.5. Comparison of normalized Lorentzian and Gaussian lineshapes.

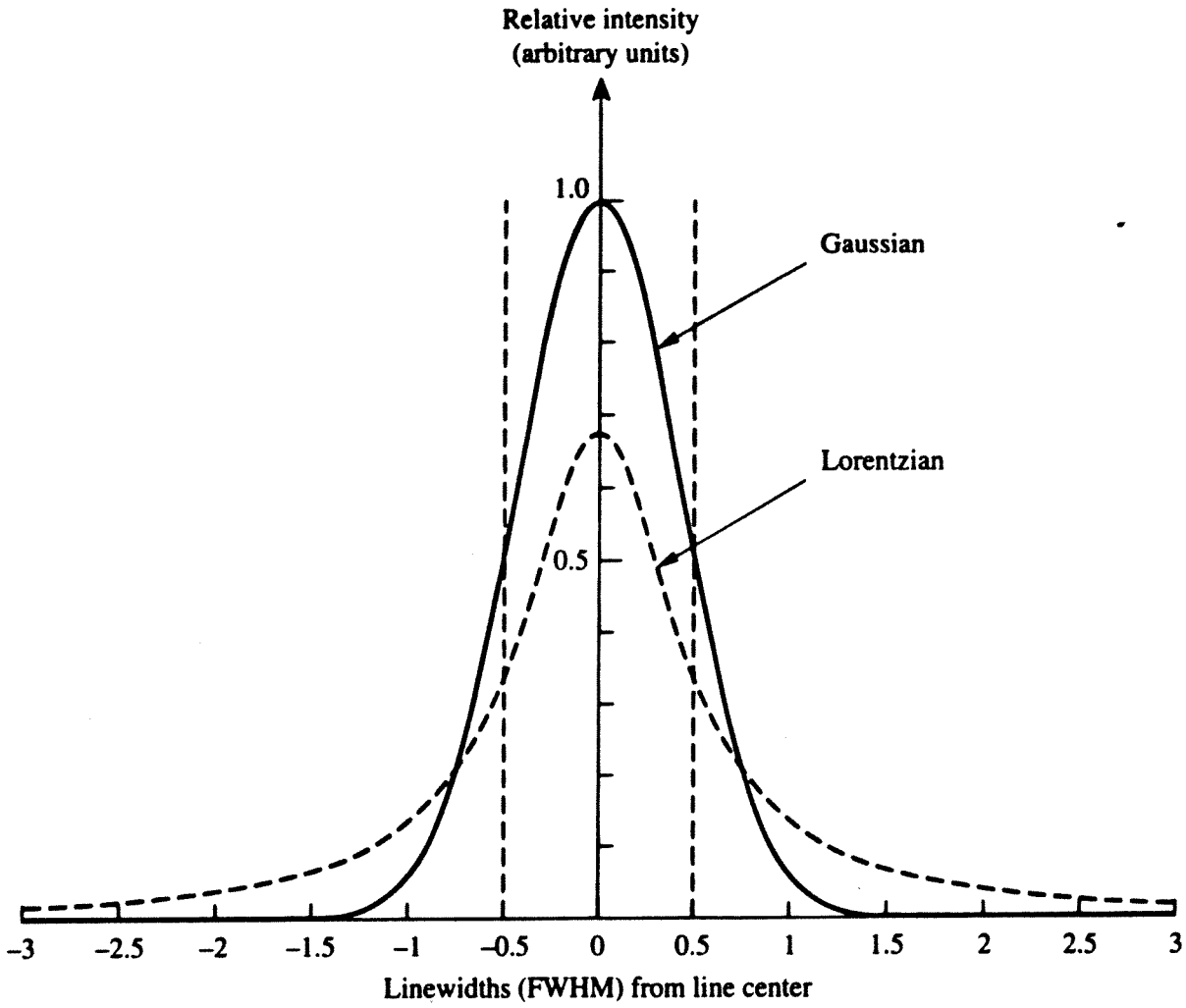

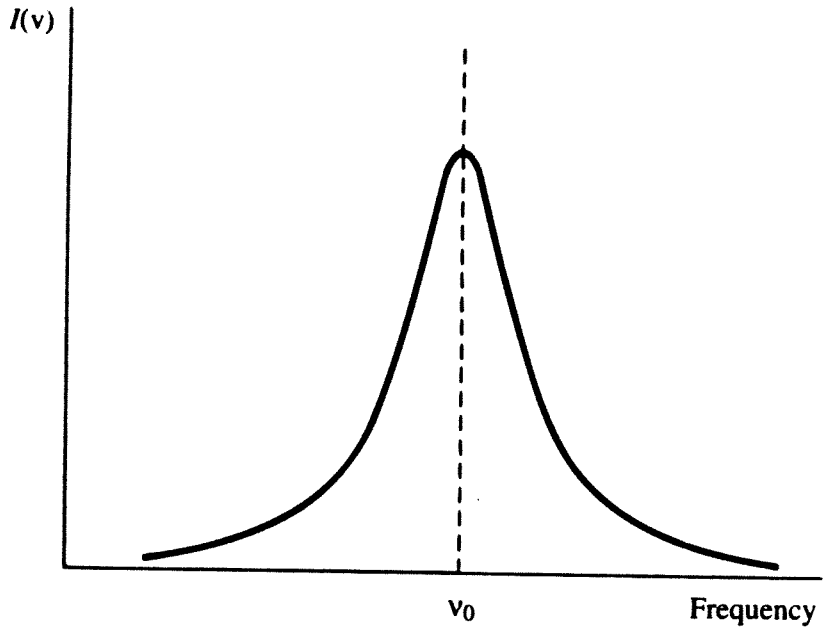

Fig. 2.6. Homogeneous broadening of a group of particles in a gas that have the same velocity.

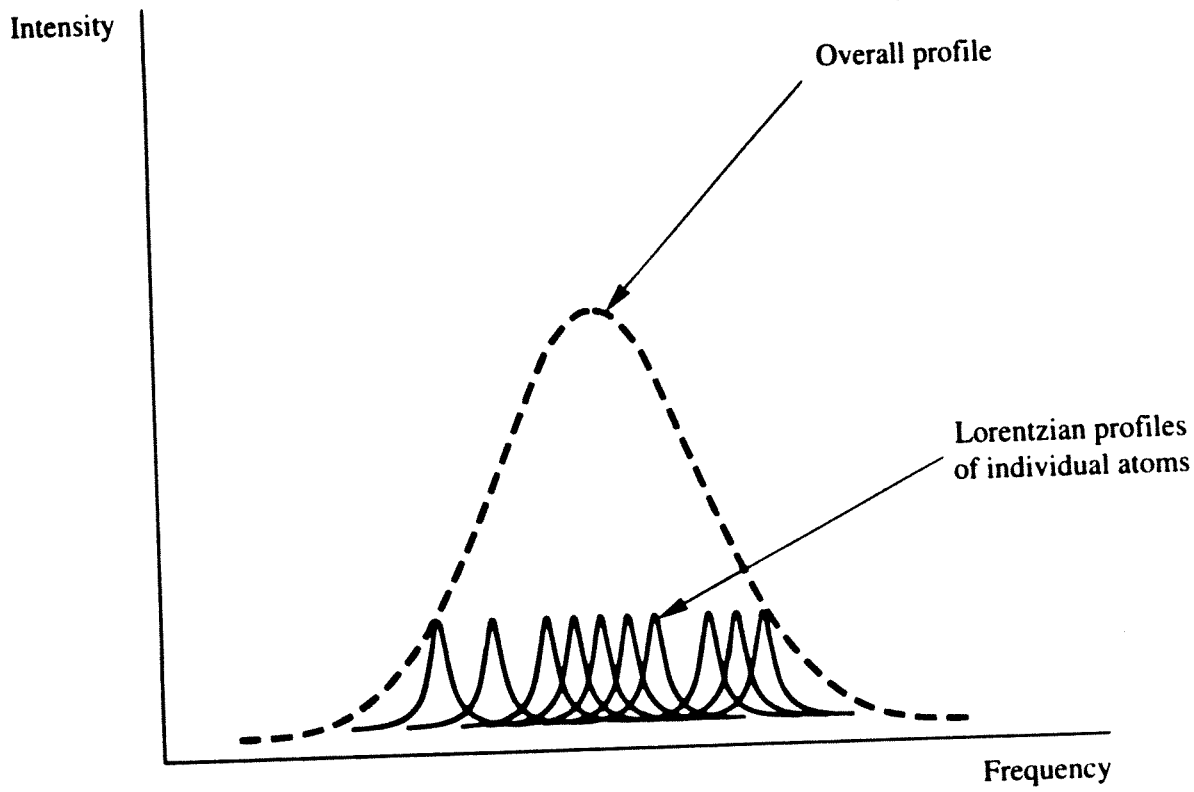

Fig. 2.7.
A Doppler-broadened distribution of Lorentzian lineshapes.

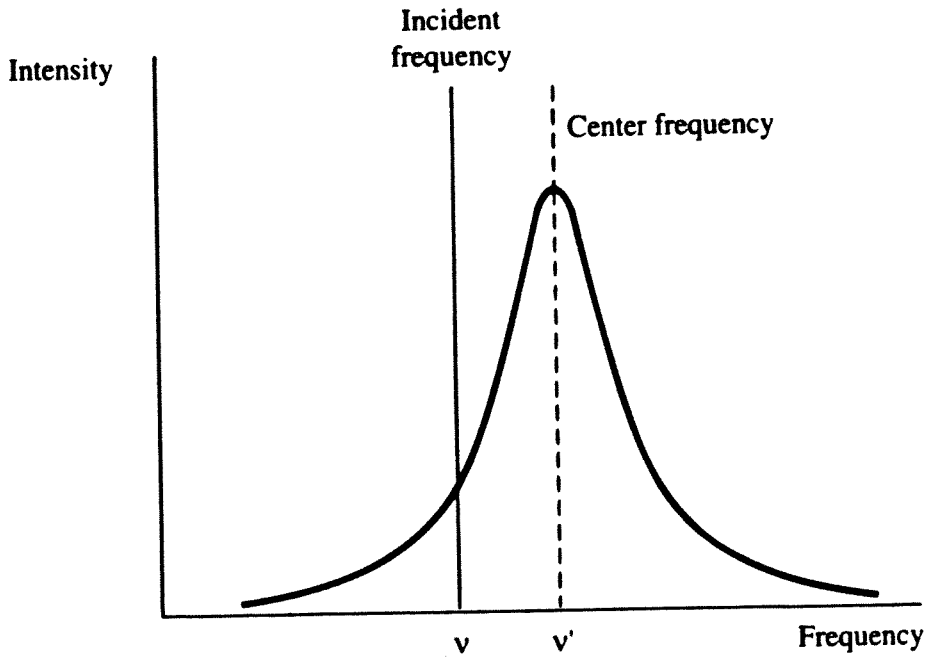

Fig. 2.8. A monochromatic field interacting with a homogeneously broadened lineshape.

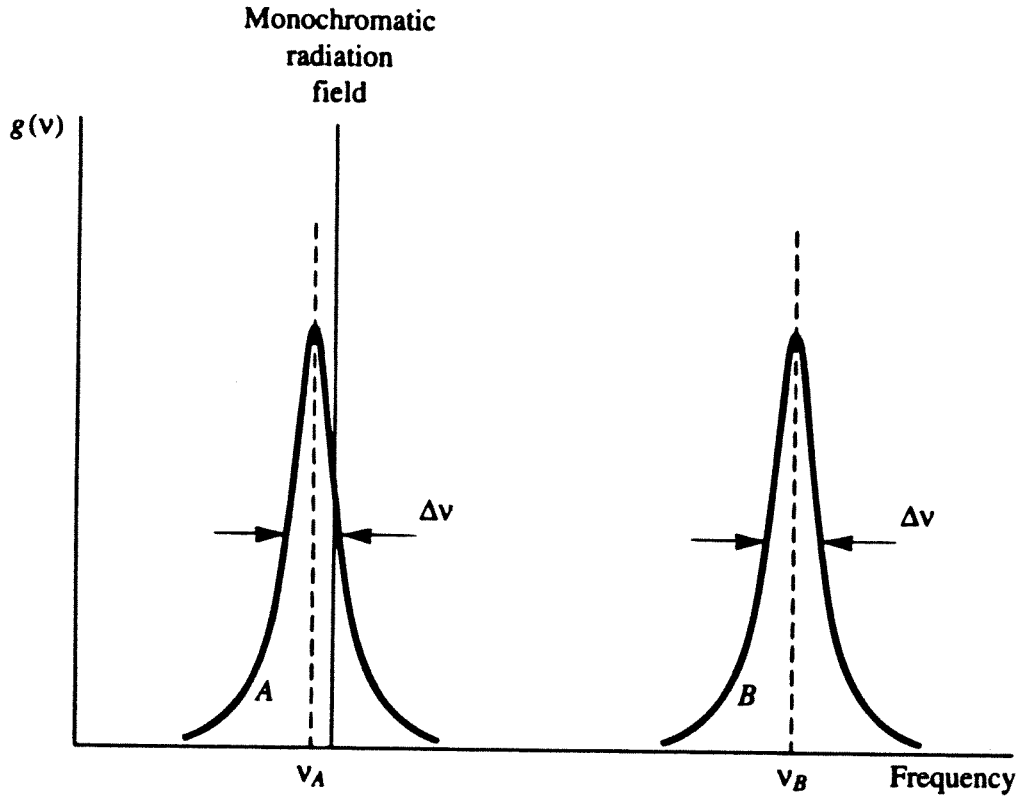

Fig. 2.9. A monochromatic radiation field interacting with two homogeneously broadened lineshapes whose center frequencies are different.

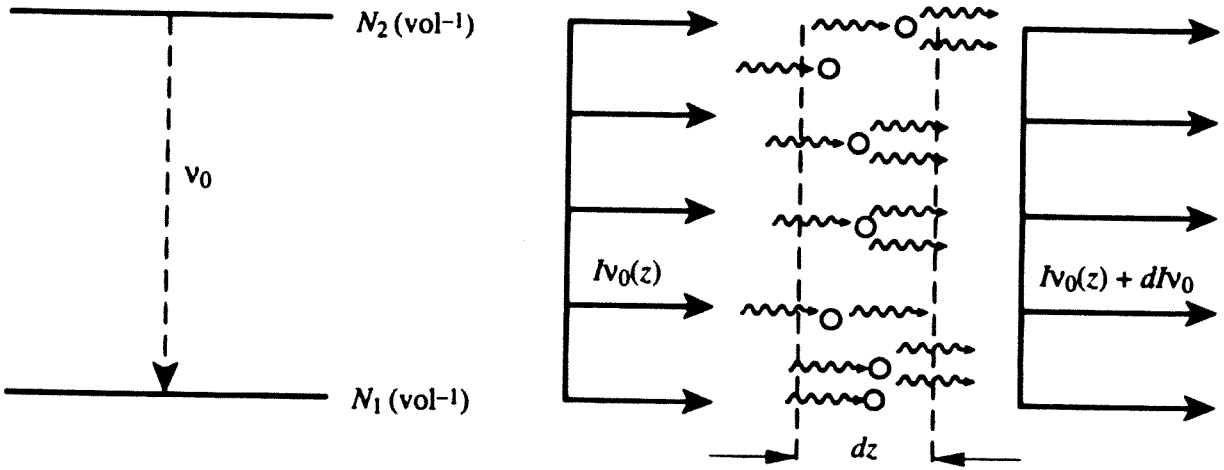

Fig. 2.10. A plane wave interacting with a collection of homogeneously broadened particles.

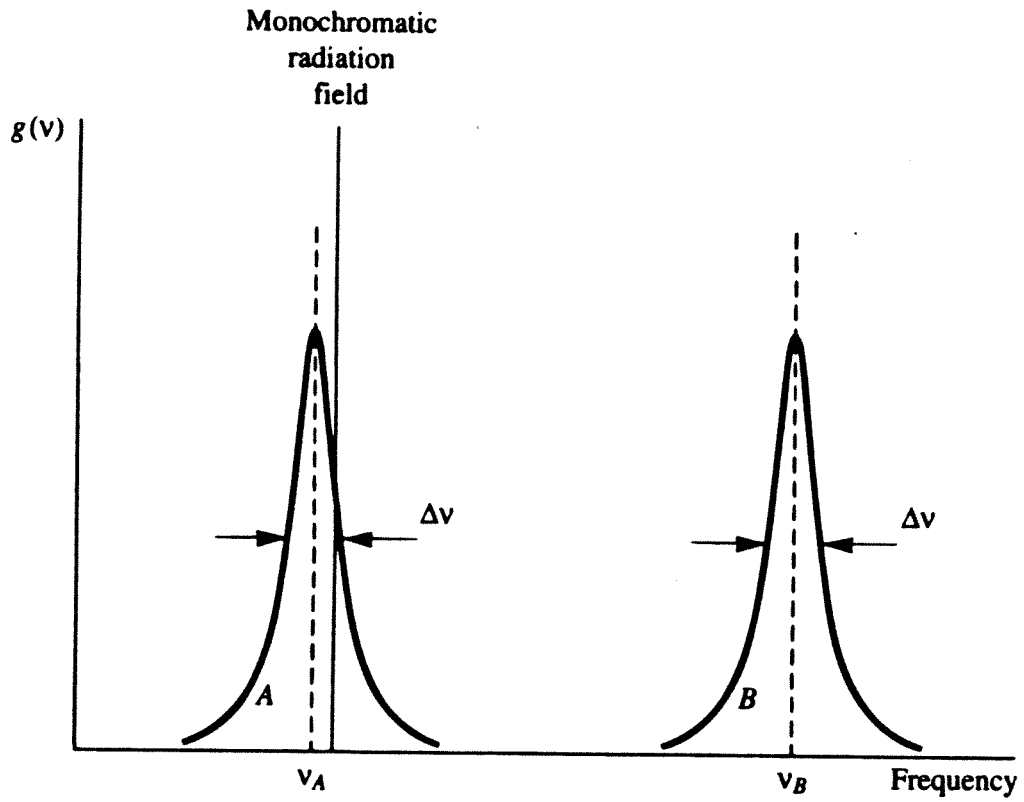

Fig. 2.9. A monochromatic radiation field interacting with two homogeneously broadened lineshapes whose center frequencies are different.

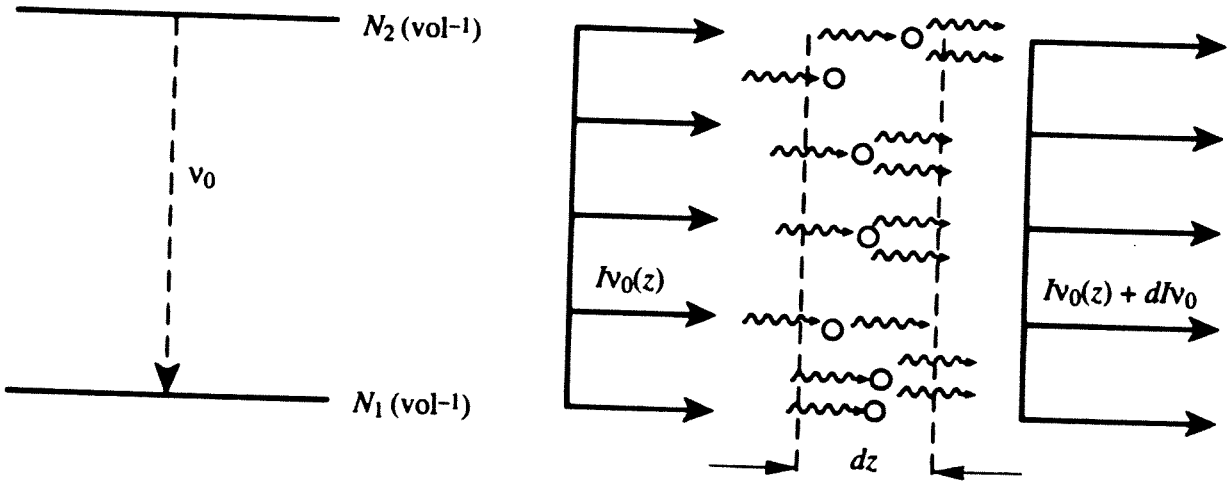

Fig. 2.10. A plane wave interacting with a collection of homogeneously broadened particles.

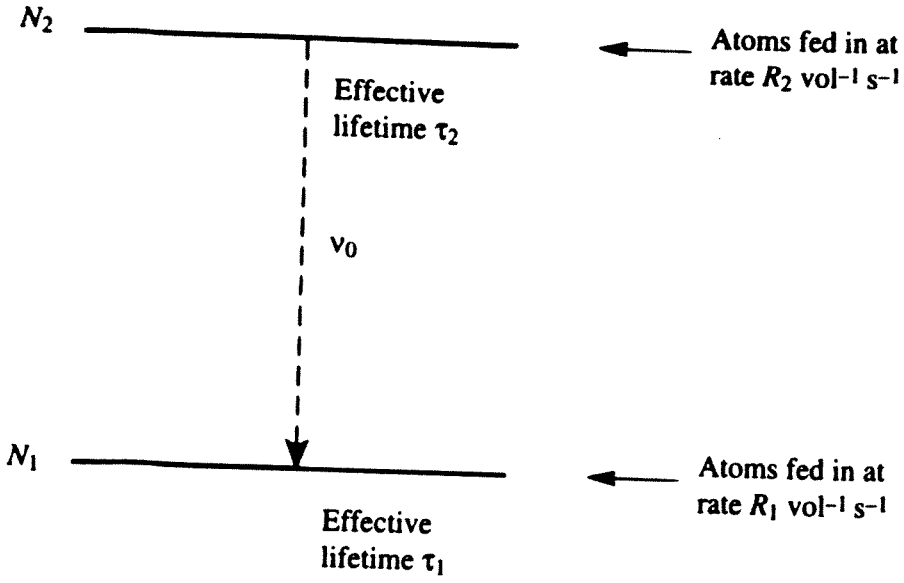

Fig. 2.11. Simple energy level system used in a discussion of amplifier saturation.

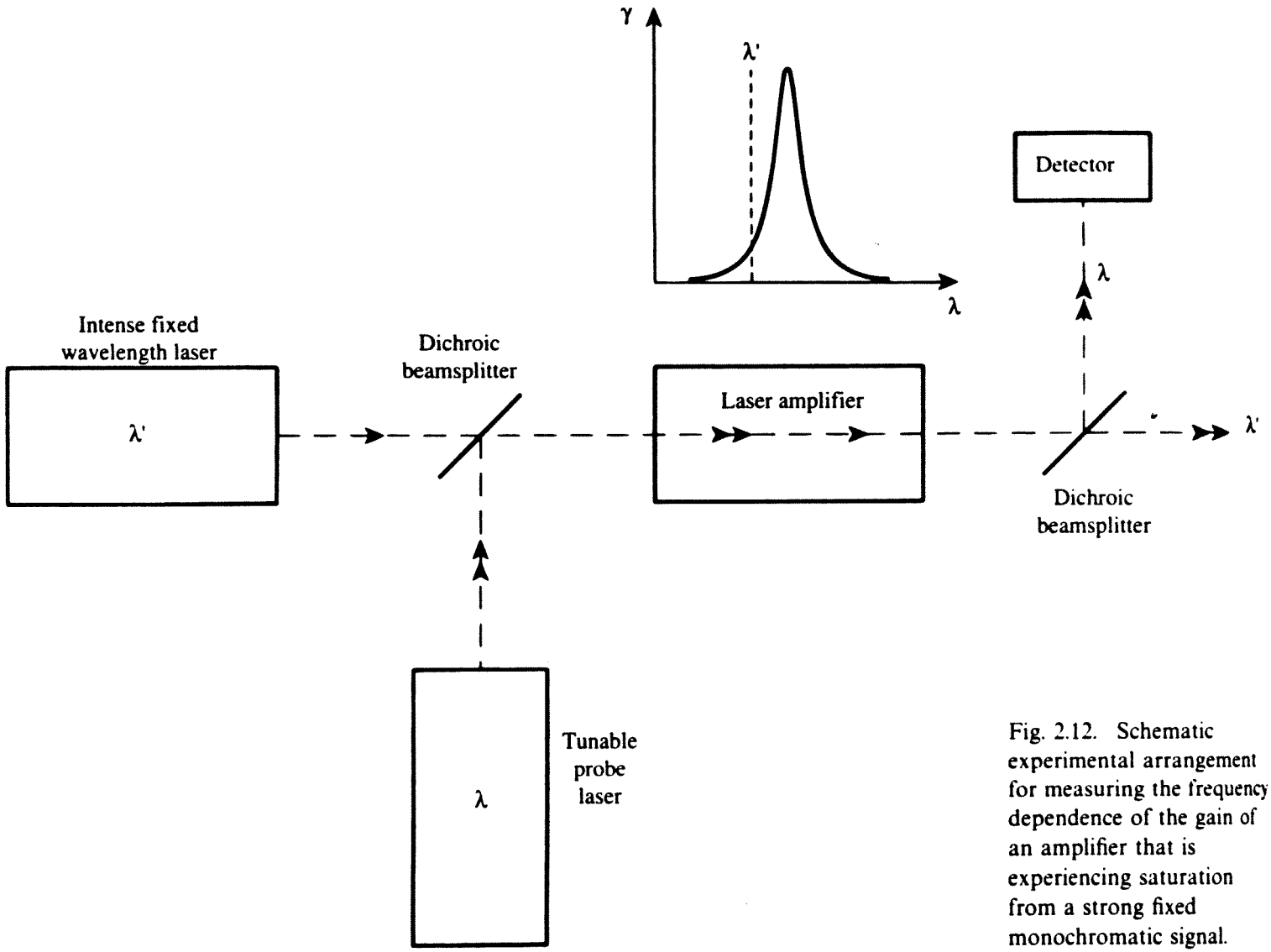

Fig. 2.12. Schematic experimental arrangement for measuring the frequency dependence of the gain of an amplifier that is experiencing saturation from a strong fixed monochromatic signal.

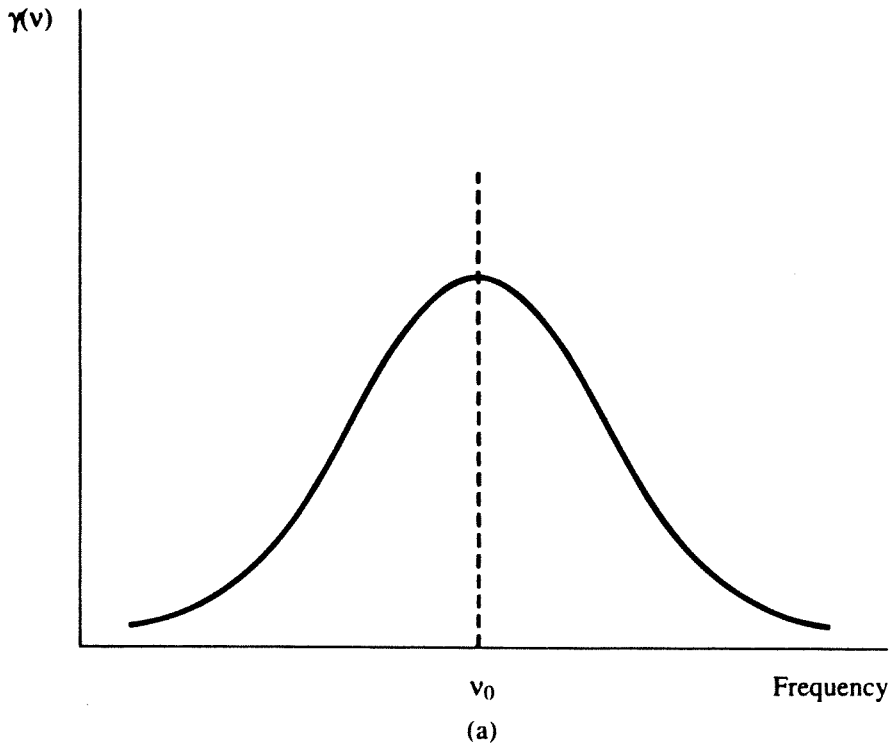

Fig. 2.13. Gain as a function of frequency in an inhomogeneously broadened amplifier. (a) Small-signal situation when no saturation has occurred. (b) Showing the production of a 'hole' in the gain curve by a strong monochromatic input at frequency ν_F.

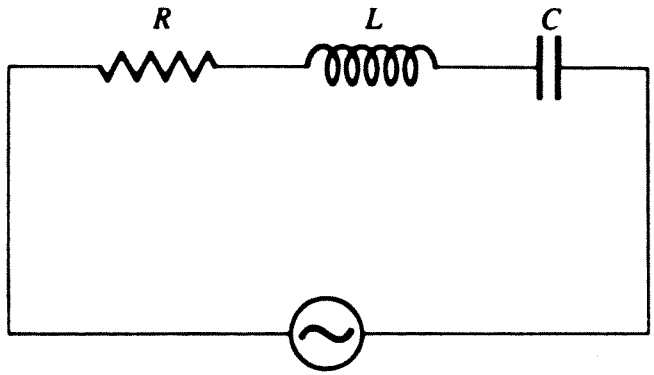

Fig. 2.14. *RLC* circuit.

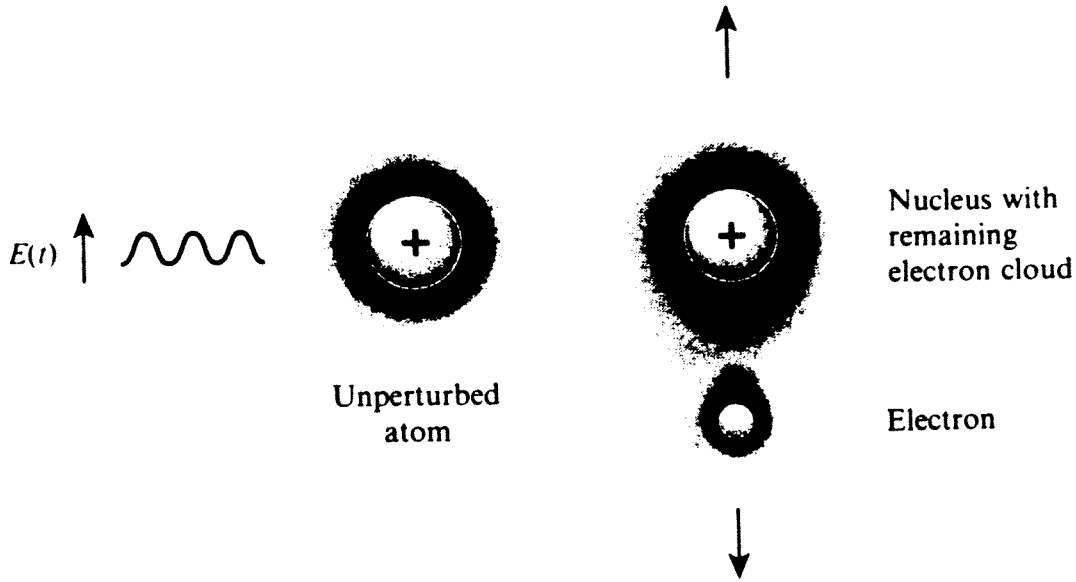

Fig. 2.15. Electron cloud and nucleus are displaced in opposite directions by an applied field.

Fig. 2.16. Frequency variation of the real, $\chi'(\nu)$, and imaginary, $\chi''(\nu)$, parts of the susceptibility calculated using the electron oscillator model.